Generation and Analysis of Tritium-Substituted Methane

D. Díaz Barrero, T. L. Le, S. Niemes, S. Welte, M. Schlösser, B. Bornschein & H. H. Telle

Published online: 25 May 2023.

Submit your article to this journal ⬈

Article views: 56

View related articles ⬈

View Crossmark data ⬈

⊛ANS®

Generation and Analysis of Tritium-Substituted Methane

D. Díaz Barrero,[a]* T. L. Le,[b] S. Niemes,[b] S. Welte,[b] M. Schlösser,[b] B. Bornschein,[b] and H. H. Telle[a]

[a]*Universidad Autónoma de Madrid, Departamento de Química Física Aplicada, 28049 Madrid, Spain*
[b]*Karlsruhe Institute of Technology (KIT), Institute for Astroparticle Physics (IAP), Tritium Laboratory Karlsruhe (TLK), 76021 Karlsruhe, Germany*

Abstract — *An unavoidable category of molecular species in large-scale tritium applications, such as nuclear fusion, are tritium-substituted hydrocarbons, which form by radiochemical reactions in the presence of (circulating) tritium and carbon (mainly from the steel of vessels and tubing). Tritium-substituted methane species, CQ_4 (with Q = H,D,T), are often the precursor for higher-order reaction chains, and thus are of particular interest. Here we describe the controlled production of CQ_4 carried out in the CAPER facility of the Tritium Laboratory Karlsruhe, exploiting catalytic reactions and species enrichment via the CAPER integral permeator. CQ_4 was generated in substantial quantities (>1000 cm^3 at ~850 mbar; with CQ_4content of up to ~20%). The samples were analyzed using laser Raman and mass spectrometry to determine the relative isotopologue composition and to trace the generation of tritiated chain hydrocarbons.*

Keywords — *Tritium-substituted methane, mass spectrometry, Raman spectroscopy, measurement and monitoring.*

Note — *Some figures may be in color only in the electronic version.*

I. INTRODUCTION

Hydrogen chemistry is very versatile and varied, and hydrogen ($^1H \equiv H$) can form molecular compounds with almost all elements in the periodic table. These are encountered in the form of ionic-bond hydrides, but also as covalent-bond compounds, like, e.g., hydrocarbon molecules, water, ammonia, etc., and in multiple metallic interactions. Hydrogen also participates in the adsorption and absorption processes, occupying interstitial voids in crystalline and metallic networks. This wealth of interactions is due to its small size and its electronic structure; note that the chemistry of its isotopes—deuterium ($^2H \equiv D$) and tritium ($^3H \equiv T$)—is equivalent, in principle.

However, for tritium (the radioactive isotope of hydrogen), one must also consider the radiochemical reactions that occur as a consequence of its β-decay $^3H \rightarrow {}^3He^+ + e^- + \bar{\nu}_e$. The highly energetic decay products, i.e., the helium ions and the β-electrons, lead to the generation of a wealth of secondary ions and radicals through impact interactions with any surrounding atoms/molecules.[1] This peculiarity of tritium modifies its chemical equilibria and reaction products with respect to the two nonradioactive isotopes (H and D), as well as the chemical kinetics of the reactions in which it participates.[2] Because of this, the products of these reactions and their concentrations are difficult to predict, in general.

In large-scale tritium applications, such as the Karlsruhe Tritium Neutrino (KATRIN) experiment[3] and the future nuclear fusion experiment ITER, as well as its successor experiments, nonnegligible amounts of short-chain tritiated hydrocarbons are generated. By and large, they contain between one and five C-atoms, which have been detected in circulating Q_2 process gases (with $Q \in$ [T, D, H]). This occurs despite the fact that these systems have gas-filtering units, such as permeation cells (or permeators), to remove unwanted non-Q_2 contaminants.

The carbon source for this type of reaction is C-extraction from the steel pipes/vessel walls, with the reactions with tritium taking place on the steel surfaces; note that it is rather unlikely that carbon originates from leaked atmospheric CO_2 or CO after passing through the permeator. Contaminating molecules need to be removed from the process gases because they may cause operational problems in large installations, be deposited in inappropriate places, or they may affect other processes, such as, e.g., the formation of plasmas.[4,5] In order to set up the means for the removal/elimination of hydrocarbon contaminants, it is necessary to study their chemistry and to determine their molecular structure, as well as the reactions that these molecules undergo among themselves with the surfaces and other parts of the systems exposed to them.

A good starting point for any in situ/inline study of the tritium-carbon chemistry is the generation of tritium-substituted hydrocarbons in sufficient quantities to allow one to perform precision spectroscopy on them, and thus obtain relevant analytical knowledge. The tritium-substituted methane species, CQ_4 (with $Q \in$ [T, D, H]) are of particular interest since, in general, they constitute the dominant species in tritium circulation systems.[5] It should also be noted that CQ_4 may serve as precursors for forming chain hydrocarbon molecules.

Despite being studied for quite some time, detailed spectroscopic knowledge about tritiated methanes is still sparse; this is because the available information corresponds to very low concentrations and very small sample quantities (see, e.g., Refs. 1,6, and 7). In those experiments, mixtures of methane and tritium were left to react for up to a few days, and the final products were analyzed by mass spectrometry and Raman spectroscopy.

In order to overcome the problem of only minute amounts of tritiated CQ_4, we utilized their production in sufficient quantities for high-resolution laser Raman spectroscopy in the CAprice PERmcat (CAPER) facility[8] at the Tritium Laboratory of Karlsruhe (TLK). Quantities of >1000 cm^3 at ~850 mbar, with a CQ_4 content of up to the order of ~20% (conservative estimate), were produced under controlled conditions. In this paper, we describe the production procedure and the detailed analysis of the samples using mass spectrometry and Raman spectroscopy.
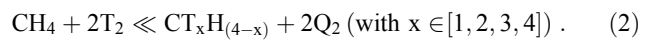
II. EXPERIMENTAL

II.A. System Fundamentals

The aim of this experiment was to produce CQ_4 as pure as possible and in sufficient quantities for precision analysis. Based on the aforementioned experiments, we knew that the production of a chemically pure compound was not possible when relying on the hypothetical isotope exchange reaction in a simple binary mixture of gases, i.e.,

$$CH_4 + 2T_2 \leftrightarrow CT_4 + 2H_2 \ . \tag{1}$$
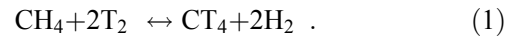
The reactions that actually take place are chemical equilibria that result in a set of products in which the H-atoms in methane are gradually replaced by T-atoms. A quasi-stable state is reached when the concentrations remain relatively constant over long periods of time, mainly consisting of the chemical family of CQ_4, in our case $Q \in$ [T,H]:

$$CH_4 + 2T_2 \lll CT_xH_{(4-x)} + 2Q_2 \ (\text{with } x \in [1,2,3,4]) \ . \tag{2}$$

Unfortunately, in the presence of tritium, equilibria are not stable but continue to evolve over time due to the tritium activity. If any mixture is stored for a long time, e.g., 18 months in the case of the experiments carried out by McConville and Menke,[1] the observation is that the tritium and carbon concentrations in the gas phase diminish and "deposits" on the surfaces of the sample containers occur. In fact, one could argue that hydrocarbons "polymerize" at the surface. Indeed, such deposits were observed in our experiments, specifically on the windows of the Raman cell used in the analysis setup, although they appeared over much shorter timescales than those reported by McConville and Menke.[1] Note, however, that little substantiated information is available on the nature of such deposits.

Unlike in previous experimental work, we deliberately altered the chemical equilibria to shift and direct them toward the product of highest interest, namely CT_4. As such, our procedure was completely different than that utilized in earlier experiments. Instead of relying on "passive" exchange reactions and associated equilibration, we used the CAPER facility to perform "catalysis-driven" synthesis.

Here it is worthwhile to recall some construction and operational features of CAPER; for details see, e.g., Ref. 8. CAPER was conceived as the experimental verification of the processing of the tokamak exhaust processing concept for ITER, whose absolute requirement was that the maximum tritium concentration in the flue gas is less than ~3.7×10^{10} Bq/m^3. Note that in terms of tritium concentration, this corresponds to the reduction of the tritium concentration by a factor of ~10^6.

CAPER achieves this in three steps in batch operation. In the first step, the effluent gases pass through a Pd/Ag membrane that is 100% selective for Q_2 in the permeator, where Q_2 (with $Q \in [T, D, H]$) is separated from molecular impurities. Two effluent streams are generated, one containing nearly all of the Q_2 (for later enrichment of tritium), and one in which the non-Q_2 contaminants are removed. In the second step, these contaminants are processed in a closed loop using a combination of heterogeneous catalysis and permeation to extract the Q_2 resulting from the catalysis. The third step is carried out in the PERMCAT reactor,[9] which simultaneously combines the permeation through the Pd/Ag membrane and the catalytic bed in a so-called "isotopic swamping" process, as used in tritium processing for the removal of impurities from the process gas.[9,10]

The use of the CAPER facility allowed us to incorporate heterogeneous catalysis into the synthesis of CQ_4 through the isotope exchange reactor containing a suitable catalyst. A second important feature of CAPER is that it provides the capability to regulate the flow rates of reagents fed into the reactor. In addition, the permeator provides the possibility of selectively eliminating products of the isotopic exchange reaction, namely Q_2. In this way, one is able to move the reaction equilibrium in the direction of interest, i.e., ultimately increasing the concentration of CQ_4 in the final mixture.

Among the other interesting features, catalysts have the ability to direct the reaction toward certain products as well as to improve the reaction kinetics, thus significantly reducing reaction times. The catalyst used in the study described here is a commercial nickel catalyst on Kieselguhr (a porous diatomaceous earth substrate used as a support for catalysts to maximize a catalyst's surface area and activity), with an approximate nickel content of 50%. In general, this type of catalyst is used for methane cracking.

The proposed mechanism of action of the aforementioned type of catalyst is the formation of carbon filaments on the active centers of the catalyst.[11]

As methane comes into contact with the catalyst, carbon chains grow, keeping nickel at the tip, which sustains the catalysis. The diffusion of carbon on the surface of the catalyst generates carbon deposits that end up deactivating its catalytic action. The operational recovery of this type of catalyst is carried out using hydrogen, among other substances. Hydrogen adsorbs reversibly on nickel, occupying active centers and displacing carbon. It competes with it for the active centers and decreases the efficiency of the cracking reaction, and thus the carbon deposits. Exploiting these two processes, the

chemical environment of the catalyst can be modified to either activate or reduce it. Note that, in our case, we used tritium instead of protium.

Hence, if the catalyst has been previously saturated with T_2, CH_4 will be retained at its surface; therefore, the isotope exchange reactions will be favored instead of the cracking reactions,[10] thus yielding $CT_xH_{(4-x)}$.

II.B. Sample Preparation

Before starting each step of the synthesis, the catalyst has to be activated and reduced so that it is in optimal condition to produce the exchange reaction. For this, a stream of high-purity T_2 (>97%) is passed through the system for at least 18 h at a temperature of 375°C to 400°C. In order to try to minimize the presence of longer-chain hydrocarbons in our samples, the synthesis process proceeds in several stages, as can be seen in the three parts of Fig. 1. The key elements involved in the synthesis are (1) two vessels for high-purity tritium and for the collected reaction mixture, respectively, (2) the permeator, and (3) the exchange reactor. Note that the valves highlighted in green are open and allow for the passage of gases, and those highlighted in white are closed, and thus block passage. Note also that the valve marked SCV constitutes a unidirectional stop-check valve assembly with backflow protection to prevent contamination of the T_2 vessel.

The reaction mixture obtained in each step is retained, as it becomes the starting reagent for the following step. Note that here we refer to the last synthesis run in a series of optimizing trials; the data shown in this paper are from this specific attempt. The relevant CAPER configurations for the substep producing samples 1, 2, and 3 are shown in the top, center, and bottom parts of Fig. 1, respectively.

Accordingly, the starting sample 1 was prepared using a flow rate of CH_4 of ~0.25 mol/h (of purity >99.99%). This flow was mixed with tritium prior to entering the reactor; its flow rate was ~4 mol/h, with tritium purity >97%. The reactor feed was maintained for ~1 h at a temperature of 375°C to 400°C.

In continuous operation, the reaction products were pumped to the permeator where the compounds $Q_2 = T_2$, HT, and H_2 were separated from the mixture. The non-Q_2 remainder was transferred to the CQ_4 vessel and stored for the next stage of the synthesis.

Note that with the partial extraction of Q_2 from the mixture, the exchange reaction becomes favorable for the generation of CQ_4 because (1) it shifts the equilibrium toward the products, avoiding the backward reaction toward the reformation of CH_4 [see Eq. (2)], and (2) it reduces the

Fig. 1. Simplified schematic diagram of the CAPER subsections used in the production/enrichment of CQ₄ (note that under certain reaction conditions, longer-chain T-hydrocarbons are generated as well). The gas circulation paths for the individual, sequential phases are indicated by arrows; they are determined by closing/opening relevant valves. The valve marked SCV is the unidirectional stop-check valve assembly. For further details, see text.

volume of the sample while increasing the fraction of CQ_4 in the sample. Note also that in order to keep sample 1 at tritium saturation conditions and to favor the isotopic exchange reaction, for storage it was diluted to 50% with high-purity T_2 (>97%).

The production of sample 2 starts with the diluted sample 1; the relevant gas circulation path is shown in the center part of Fig. 1 (note that in this procedural step the permeator is bypassed). In this second step, the gas mixture passes only through the reactor; the reaction time and temperature conditions of the reactor were kept the same as in the first step. All gases leaving the reactor were collected in the CQ_4 vessel to be used in the third step of the synthesis.

The path for the production of sample 3 is shown in the lower part of Fig. 1. The mixture from the previous stage (sample 2) was fed back into the exchange reactor and more tritium was added at a flow rate of ~6 mol/h. Circulation was maintained for ~3 h, keeping the same temperature conditions as before. Note that now, with the permeator in the loop once more, the reaction products were separated into two effluents again; i.e., Q_2 and CQ_4 are directed toward their respective vessels for storage.

Overall, about 0.21 mol of product gas mixture was generated, which is equivalent to ~5 × 10^3 cm^3 for standard pressure and temperature conditions. This was more than enough to conduct an extensive series of analytical measurements to characterize the gas composition and to record high-resolution Raman spectra.

II.C. Measurement Protocol

At each step of the synthesis, aliquots of the three produced samples were transferred to tritium-compatible Raman cells and sample cylinders; these were transferred to the TRIHYDE facility of the TLK for analysis. Note that TRIHYDE is a tritium-compatible system designed for gas mixing and analysis. It incorporates a range of measurement system devices, including high-resolution laser Raman spectroscopy and mass spectrometry.[12] The samples were measured immediately after they were prepared and were not stored; thus they should constitute a reliable snapshot of the concentrations and majority species at each stage of the synthesis.

First, the Raman spectra were measured using the TRIHYDE-incorporated laser Raman (LARA) measurement instrument. This is assembled around a glove-box appendix[13] containing the Raman sample cell. It comprises a green diode-pumped solid-state laser (GEM, Laser Quantum), with an emission wavelength of λ_L = 532 nm, continuous output power of P_L = 2 W, and Raman light collection at 90 deg with fiber-bundle coupling to the Raman spectrometer (SP2150 spectrograph with Pixis400B CCD detector, Princeton Instruments).

All of our Raman cells had the same volume of ~7 cm^3; they were filled to around ~850 mbar of sample gas. Note that for the Raman spectral data shown in Fig. 2, 20 spectra of 90-s accumulation time each were recorded (and averaged) in the spectral range of interest of 1500 to 4200 cm^{-1}.

After completion of the Raman measurements, the sample gas was bled from the cell into the mass spectrometer (quadrupole residual gas analyzer HPQ3S, MKS Instruments Inc.) via inlet dosing (UDV 040, Pfeiffer); the measurement pressure was adjusted to about 10^{-4} mbar. In the instrument range 1 to 100 atomic mass units (amu), 50 individual spectra of 30-s accumulation each were recorded (and averaged); these mass spectral data are discussed later in Sec. III.B.
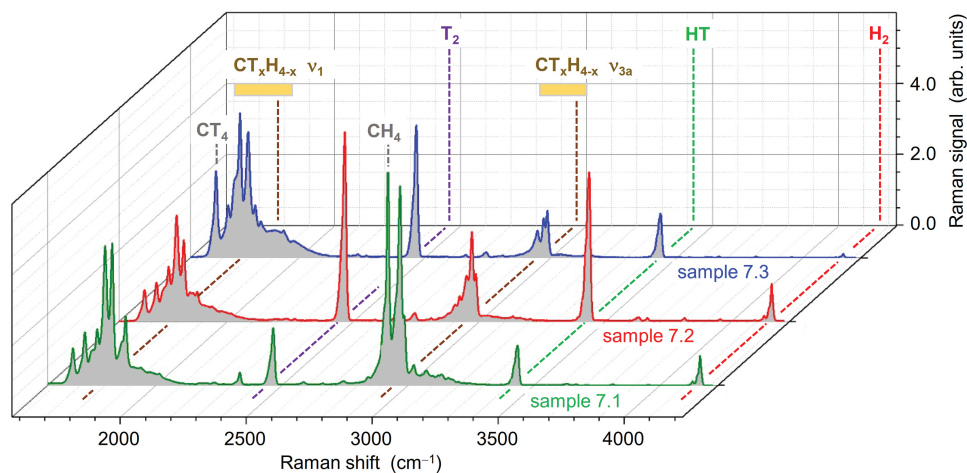

Fig. 2. Data of the analysis of the Raman spectra for the sequence samples 1, 2, and 3 recorded after the individual CQ_4 enrichment steps; for details, see text.

III. RESULTS

III.A. Raman Spectroscopy

The sequence of spectra from the start of the catalytic $CH_4 + T_2$ synthesis (sample 1) to its end (sample 3), shown in Fig. 2, reveals three distinct series of features, which we discuss separately.

First, all three spectra contained the characteristic Q_1 branch lines of the molecular hydrogen isotopologues expected for this type of synthesis, i.e., from T_2 (at ~2466 cm^{-1}), HT (at ~3435 cm^{-1}), and H_2 (at ~4159 cm^{-1}). Their amplitudes differed significantly, indicating the evolution of concentrations for these molecular constituents. While T_2 was present in the starting mixture by default, HT and H_2 are products generated during the synthesis reactions. The source for the generation of these hydrogen isotopologues was CH_4, in which H-atoms were substituted by T-atoms in the course of the isotope exchange reactions. Thus, in the Raman spectrum corresponding to the initial sample 1, the Raman peak corresponding to the v_1 band of CH_4 also can be observed (at ~2919 cm^{-1}).

This peak diminished as the synthesis progressed; already in the spectrum for sample 2, it had almost completely disappeared, with CH_4 increasingly being converted into $CT_xH_{(4-x)}$. Note the spectral bands displaced toward the larger Raman shift relative to CH_4 v_1; these are associated with the v_{3a} bands of the tritium-substituted methanes. Note also that the highest content of T_2, HT, and H_2, with respect to the rest of the species present in the mixture, was observed for sample 2. This is because during its preparation the permeator was bypassed, which otherwise would have largely removed Q_2 from the mixture.

The set of Raman spectral features in the range 1650 to 1900 cm^{-1} is dominated by the contribution from the symmetric, normal vibrational mode v_1 of the $CT_xH_{(4-x)}$ family. Note that the peak of the fully tritiated methane, CT_4, increases at the expense of the other T-methane species as the gas mixture passes through the catalyst and the permeator removes the Q_2 products from the medium, thus preventing hydrogen from reverse substitution.

For further, semiquantitative interpretation of the spectra, one should recall that the Raman signal S_R can be approximated by the simplified expression

$$S_R \propto \widetilde{v}_L \, \widetilde{v}_R^3 \cdot \Phi_{if} \cdot N_i \cdot I_L \ , \tag{3}$$

where

$\widetilde{v}_L$ = laser transition energy

$\widetilde{v}_R$ = Raman transition energies

Φ_{if} = Raman transition probability

N_i = molecular particle density

I_L = excitation laser power.

Expression (3) can be used to extract the relative molecular concentrations from the spectra, in principle. However, while for tritium containing Q_2, the values for the transition probabilities Φ_{if} are known,[12] those for the tritium-substituted methane species CQ_4 are not available; thus, quantitative interpretation is rather difficult at present.

For a better understanding of the evolution in the concentrations of the $CT_xH_{(4-x)}$ family, one may zoom into the v_1 region of the Raman spectra, as shown in Fig. 3.

After the first passage of the sample gas through the catalyst reactor, the predominant species in sample 1 are those with the highest hydrogen content, i.e., CTH_3 and CT_2H_2; but already a substantial quantity of CT_3H has been generated, together with smaller amounts of CT_4.

In the preparation of sample 2, during which the gas mixture passes through the catalyst for a second time but bypasses the permeator, the T-methane species, which dominated in sample 1, start to diminish, along with the
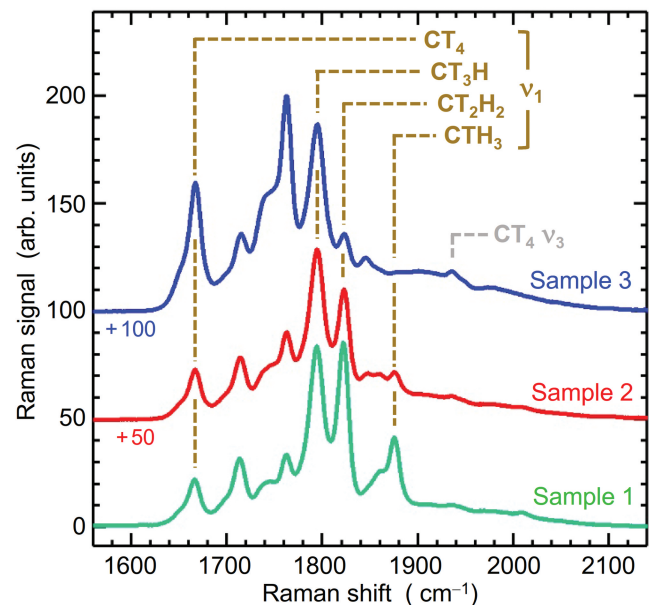

Fig. 3. Detail of the group of peaks corresponding to the symmetric normal mode of vibration v_1 of the $CT_xH_{(4-x)}$ family of compounds.

initial reagent CH_4. Conceptually, this is not surprising. Recall that for the second step, sample 1 was diluted to 50% in high-purity T_2. Thus, the dominant species in the chemical environment of both the catalyst and the gas mixture is tritium. Consequently, the action of the catalyst and the balancing with surplus tritium drive the active centers toward saturation with tritium, i.e., effectively exchanging most H-atoms with T-atoms.

In the last step of the synthesis, i.e., in generating sample 3, the relative concentration for the species of highest interest, CT_4, increases by almost a factor of 3 with respect to the previous phase. The two main reasons for this increase are as follows:

1. The gas fed to the reactor in this phase shows CT_3H as the majority species within the $CT_xH_{(4-x)}$ family, and thus a significant fraction of exchange reactions yields CT_4.

2. The circulation time, and thus the time available for exchange reactions, is three times longer than in the two previous phases.

The nearly linear relation between the growth in the CT_4 concentration and the time over which exchange reactions progress invites the notion that, at least on the timescale of the experiments discussed here, it is the catalytic conversion that dominates and the influence of tritium decay on the reactions may be treated as being secondary.

It should be stressed that the synthesis process critically depends on the state of the catalyst. For this, optimal reaction conditions of the catalyst (activated or reduced) need to be established at the beginning of each phase. Of equal importance is that an optimal reaction environment in the medium be maintained, i.e., that fresh high-purity T_2 needs to be injected and that the products HT and H_2, generated by the catalysis reactions, are removed. By this means, the catalyst remains in optimal conditions for longer, and the reaction favors the increase of tritiated methanes.

If the catalyst does not operate under optimal conditions, it would likely deactivate. This would result in mixtures containing lower concentrations of $CT_xH_{(4-x)}$ (CT_4 in particular) and higher amounts of hydrocarbon chain molecules; this was observed in some of our earlier synthesis attempts.

III.B. Mass Spectrometry

With regard to the molecular isotopologues Q_2, it can be seen that sample 2 is the one with the highest quantity of T_2 (at 6 amu), HT (at 4 amu), and H_2 (at 2 amu), and their atomic fragments, as was the case for the Raman spectroscopic data shown in Fig. 4.

For the family of tritium-substituted methane molecules, $CT_xH_{(4-x)}$, the mass spectra show that while all members of the family are present, (semi-) quantification becomes somewhat complex in contrast to the Raman data. This is because of fragmentation into "daughter" molecules in which successively Q-atoms are stripped from the "parent" molecule, leading to the same daughter molecules from different parent molecules. Overall, feature-rich mass spectra result if many, or all, $CT_xH_{(4-x)}$ parents are present in the gas mixture (for mass spectral patterns see Ref. 14).

For sample 1, for which hydrogen is still plentiful, all $CT_xH_{(4-x)}$ parents and their daughter products are observed, giving rise to a series of incremental mass peaks ($\Delta m = 1$ amu) ranging from atomic carbon, C (12 amu),
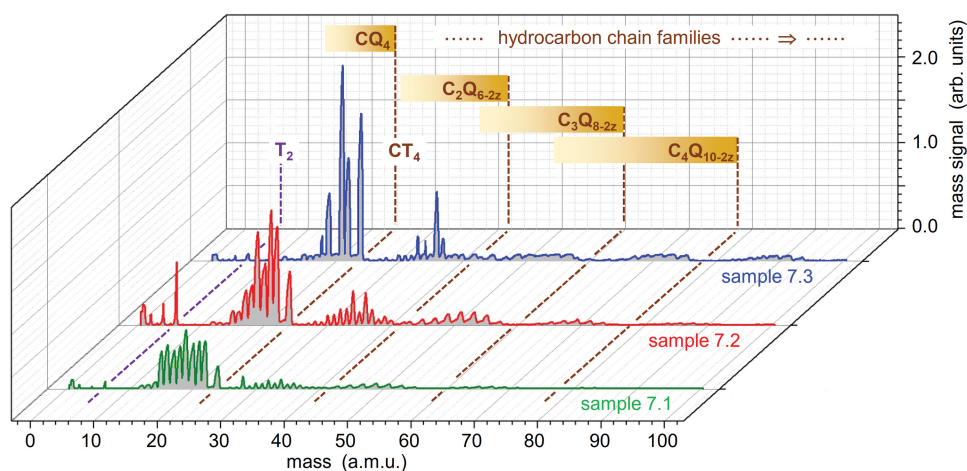

Fig. 4. Data of the analysis of the mass spectra for the sequence samples 1, 2, and 3 recorded after the individual CQ_4 enrichment steps; for details, see text.

to fully tritiated methane, CT_4 (24 amu). The exception is mass 23 amu, for which neither a parent nor a daughter fragment of $CT_xH_{(4-x)}$ exists. As the synthesis process progresses, the mass spectra become sparse, until for sample 3, basically only two parents and two of their daughter fragments prevail, namely, CT_4 (24 amu)/CT_3 (21 amu) and CT_3H (22 amu)/CT_2H (19 amu). This confirms the findings from the Raman spectra quite well.

It is worth noting that the aforementioned filament phenomenon manifests itself in the mass spectra, too. As the overall interaction time between the catalyst and the mixture increases, so does the concentration of carbon chain molecules (number of C-atoms n > 1). These can be saturated hydrocarbons, i.e., $C_nH_{(2n+2)}$ (with only C–C single bonds in the chain ≡ alkanes); unsaturated hydrocarbons, i.e., C_nH_{2n} (with one C=C double bond in the chain ≡ alkenes); or $C_nH_{(2n-2)}$ (with one C≡C triple bond in the chain ≡ alkynes). Of course, more than one unsaturated bond may be encountered, giving rise to a range of additional hydrocarbon families.

For the particular family of molecules with two C-atoms (n = 2), $C_2Q_{(6-2z)}$ (with z indicating the number of unsaturated bonds), the following interesting feature is observed. In the mass spectrum of sample 3, the peak with mass 36 amu stands out, exhibiting quite a large amplitude that has evolved over the duration of the synthesis process. It can be assigned to the chemically rather stable molecule C_2T_4, i.e., fully tritiated ethylene. While exact quantification was not possible, its concentration seems to be substantial in comparison to the signal amplitudes of the other hydrocarbon molecules. This leads us to think that some of the lower-intensity Raman peaks, which we have not yet identified in the spectra, might actually originate from the aforementioned C_2T_4.

IV. DISCUSSION

As suspected, quite from the beginning a chemically pure compound could not be obtained (in principle we had wished for "pure" CT_4). However, the multistep synthesis strategy did allow us to shift the chemical equilibria and direct the reaction products toward the species with the highest tritium content, the majority being CT_3H and CT_4 with almost similar magnitude (compare the amplitudes in both the Raman spectra shown in Figs. 2 and 3). The concentrations of the different species can be estimated from the Raman spectral data; by and large, these were corroborated in the mass spectrometry analysis.

As stated earlier, the species concentrations can be reasonably well quantified from the (integrated) Q_1 branch Raman data based on Eq. (3). However, for this the Raman transition probabilities Φ_{if} for each species need to be known. Unfortunately, these are not known for the tritium-substituted methanes. Regardless, one can make at least a crude estimate for the CQ_4 content in sample 3. Using the observed relative transition probability Φ_{rel} for the non-tritiated species CH_4 (with $\Phi_{rel}(CH_4) = 6.0$) and H_2 (with $\Phi_{rel}(H_2) = 2.4$) (Ref. 15), and assuming that $\Phi_{rel}(CH_4) \approx \Phi_{rel}(CQ_4)$, one can estimate the CQ_4-content of sample 3 to be ~20%. From this estimate, the yield for this isotope exchange reaction, i.e., for the conversion of CH_4 to CT_3H and CT_4 (the two majority species in the resulting mixture), is approximately ~16%.

It should be possible to improve this yield by tweaking the synthesis design to keep the catalyst in better activation and reduction conditions. This might be done either (1) by decreasing the flow rate feeding the exchange reactor or (2) by finding strategies to more effectively prevent the formation of carbon filaments on the catalyst. It is in these amorphous carbon filaments where most of the CH_4 introduced into the system in the first step of the synthesis is lost (remember that these catalysts are used precisely for methane cracking). Some of it remains on the catalyst and is removed each time the catalyst is regenerated between synthesis steps. Some of the filament fragments were observed in the mass spectra as the families of $C_3Q_{(8-2z)}$, $C_4Q_{(10-2z)}$, $C_5Q_{(12-2z)}$, etc.

Both the amount of the mixture (~5-6 × 10^3 cm^3) and the concentration of $CT_xH_{(4-x)}$ were significantly higher than those utilized in previous studies. This gave us the opportunity to record Raman spectra with further increased resolution in order to isolate individual Q_1 branches of the symmetric normal mode of vibration v_1 of each of the species present in the mixture. With this one should be able to estimate the amount of each of them more rigorously.

V. CONCLUSION

Our results show that CQ_4 can be produced in large enough quantities from an individual production batch so that one can perform precision spectroscopy on them, and thus obtain relevant analytical knowledge. Therefore, a wealth of experiments can be performed using the same starting sample. Such experiments may address aspects of different analysis techniques (as demonstrated here), or the gas may be used for specific chemical interaction scenarios, such as, for example, exposure of particular surfaces to tritiated methane. But this work also shows that our approach, while rather successful, is still not yet perfect.

Since the production of CQ_4 via the CAPER facility had to compete with its priority use for the KATRIN experiment, the time available for incremental improvements of the CQ_4 processing procedures was rather limited. However, with the experience gained thus far, we envisage coordinating our future efforts better with the KATRIN service periods during which CAPER can be utilized for different tasks. In this way, we expect to gain even better control over the distribution of CQ_4 isotopologues in the mixture as was possible to date. Even better for the production of pure CT_4, which would be ideal, would be to use a H-free production path. This, however, would require the use of a different chemical reactor setup, which would be a long-term goal since at present the perpetual use of CAPER for other experiments prevents us from implementing structural changes.

Equally, our Raman analysis warrants attention as well. This is because the TRIHYDE Raman analysis tool was designed to analyze Q_2 mixtures rather than perform high-resolution spectroscopy. Thus, in particular, it is planned to add a high-resolution Raman spectrometer that would allow for full spectral resolution of all $CT_x H_{(4-x)}$ species; at present, parts of the spectral features do overlap.

In this context, we have just begun theoretical quantum calculations on the structure of the Raman vibration-rotation spectra of each species in the $CT_x H_{(4-x)}$ family. The aim is to be able to subtract these theoretical calculations from the experimental spectra in order to both reduce the non-Q_1 branch background and to better attribute the contribution of each species in the family to the overall Raman spectrum (unfortunately, individual S_1, R_1, P_1, and O_1 branches overlap and cannot be easily separated). With the help of the pure synthetic Raman spectra, in comparison to the mixed experimental Raman spectra, we hope to be able to disentangle and quantify all individual $CT_x H_{(4-x)}$ species in our gas mixtures.

Acknowledgments

Disclosure Statement

No potential conflict of interest was reported by the authors.

ORCID

D. Díaz Barrero http://orcid.org/0000-0002-1384-3950
S. Niemes http://orcid.org/0000-0001-5420-4533
M. Schlösser http://orcid.org/0000-0002-3091-8088
B. Bornschein http://orcid.org/0000-0002-2930-8549
H. H. Telle http://orcid.org/0000-0003-4839-7310

References

1. G. T. MCCONVILLE and D. A. MENKE, "Exchange of Dilute CH_4 in Tritium Gas," *Fusion Technol.*, **23**, *3*, 316 (1993); https://doi.org/10.13182/FST93-A30159.

2. R. J. KANDEL, "Methane-Tritium System. II. Kinetics of the Exchange Reaction," *J. Chem. Phys.*, **41**, *8*, 2435 (1964); https://doi.org/10.1063/1.1726283.

3. THE KATRIN COLLABORATION, "Direct Neutrino-Mass Measurement with Sub-eV Sensitivity," *Nature Phys.*, **18**, *2*, 160 (2022); https://doi.org/10.1038/s41567-021-01463-1.

4. L. DÖRR et al., "The Closed Tritium Cycle of the Tritium Laboratory Karlsruhe," *Fusion Sci. Technol.*, **48**, *1*, 262 (2005); https://doi.org/10.13182/FST05-A924.

5. M. STURM et al., "Kilogram Scale Throughput Performance of the KATRIN Tritium Handling System," *Fusion Eng. Des.*, **170**, 112507 (2021); https://www.sciencedirect.com/science/article/pii/S0920379621002830.

6. U. ENGELMANN, "Raman Spectroscopic and Mass Spectrometric Investigations of the Hydrogen Isotopes and Isotopically-Labeled Methane," Report HNF-0532, Institute for Radiochemistry, Karlsruhe Nuclear Research Center (Feb. 1997); https://www.osti.gov/servlets/purl/334155 (current as of Dec. 4, 2022).

7. T. UDA et al., "Application of Laser Raman Spectroscopy to Isotopic Methane Analysis in Fusion Fuel Gas Processing Systems," *Fusion Technol.*, **21**, *2P2*, 436 (1992); https://doi.org/10.13182/FST92-A29784.

8. B. BORNSCHEIN et al., "Successful Experimental Verification of the Tokamak Exhaust Processing Concept of ITER with the CAPER Facility," *Fusion Sci. Technol.*, **48**, *1*, 11 (2005); https://doi.org/10.13182/FST05-A870.

9. D. DEMANGE et al., "Counter-Current Isotope Swamping in a Membrane Reactor: The PERMCAT Process and Its Applications in Fusion Technology," *Catal. Today*, **156**, *3–4*, 140 (2010); https://doi.org/10.1016/j.cattod.2010.02.033.

10. M. GLUGLA et al., "Development of Specific Catalysts for Detritiation of Gases by Counter Current Isotopic Swamping," *Fusion Sci. Technol.*, **41**, *3P2*, 969 (2002); https://doi.org/10.13182/FST02-A22729.

⊗ANS

11. A. AMIN et al., "Reaction and Deactivation Rates of Methane Catalytic Cracking Over Nickel," *Ind. Eng. Chem. Res.*, **50**, *22*, 12460 (2011); https://doi.org/10.1021/ie201194z.

12. S. NIEMES et al., "Accurate Reference Gas Mixtures Containing Tritiated Molecules: Their Production and Raman-Based Analysis," *Sensors*, **21**, *18*, 6170 (2021); https://doi.org/10.3390/s21186170.

13. S. FISCHER et al., "Monitoring of Tritium Purity During Long-Term Circulation in the KATRIN Test Experiment LOOPINO Using Laser Raman Spectroscopy," *Fusion Sci. Technol.*, **60**, *3*, 925 (2011); https://doi.org/10.13182/FST11-A12567.

14. R. J. KANDEL, "Methane-Tritium System. I. Mass Spectra of Tritium-Substituted Methanes," *J. Chem. Phys.*, **39**, *10*, 2581 (1963); https://doi.org/10.1063/1.1734065.

15. W. R. FENNER et al., "Raman Cross Section of Some Simple Gases," *J. Opt. Soc. Am.*, **63**, *1*, 73 (1973); https://doi.org/10.1364/JOSA.63.000073.